Available online at www.sciencedirect.com
SCIENCE DIRECT®
Journal of Process Control 14 (2004) 617–626
JOURNAL OF PROCESS CONTROL
www.elsevier.com/locate/jprocont

Design of a stable adaptive controller for driving aerobic fermentation processes near maximum oxygen transfer capacity

R. Oliveira [a,*], R. Simutis [b], S. Feyo de Azevedo [c]

[a] *REQUIMTE/CQFB, Department of Chemistry, Centre for Fine Chemistry and Biotechnology, Faculty of Sciences and Technology, Universidade Nova de Lisboa, P-2829-516 Caparica, Portugal*

[b] *Process Control Department, Kaunas University of Technology, Kaunas LT-3028, Lithuania*

[c] *Department of Chemical Engineering, Institute for Systems and Robotics, Faculty of Engineering, University of Porto, P-4200-465 Porto, Portugal*

Abstract

In many industrial fermentation processes oxygen availability is the main limiting factor for product production. Typically the dissolved oxygen (DO) concentration decreases continuously at the beginning of the batch until it reaches a critical level where the oxygen transfer rate is very close to the vessel's maximum transfer capacity. The process may be further driven close to this sensitive operating point with a controller that manipulates the carbon source feed rate. This operating strategy is linked with important productivity issues and is still frequently realised in open-loop at production scale. The main purpose of the present study is to derive an effective closed-loop control solution and to demonstrate its economical advantage in relation to the open-loop form of operation. A stable model reference adaptive controller (MRAC) was designed based on a phenomenological model of the process. The implementation requires two on-line measurements: the DO tension and oxygen transfer rate (OTR) between gas–liquid phases, which are nowadays standard and easily available in production facilities. The controller performance is accessed with a simulation case study. The main results show that the adaptive controller is precise, stable and robust to disturbances and to inaccuracies like variability in raw materials typical in fermentations run in complex media. The controller is simple, easy to implement, and could possibly improve productivity in processes for which oxygen transfer capacity is limiting growth and product production.

Keywords: Aerobic fermentation processes; Adaptive control; Dissolved oxygen control

1. Introduction

Many industrial fermentation processes are run under carbon source limitation, this essentially meaning that the carbon source is the limiting substrate whereas all other nutrients are present in excess in the cultivation medium. For such processes, the feeding strategy of the carbon source is the most important parameter for controlling the cells metabolism and ultimately the process dynamics. In aerobic fermentations, the DO concentration must be maintained above a critical limiting level for preventing that oxygen, instead of the carbon source, becomes the limiting substrate. Since oxygen is normally consumed in large quantities and since its solubility in typical fermentation medium is very low, it must be supplied continuously by aeration.

The DO concentration is routinely regulated to constant levels by manipulating the stirrer speed and/or inlet airflow rate. This control strategy is feasible if the oxygen transfer rate (OTR) from gas bubbles into the liquid phase is higher than the metabolic oxygen consumption. Unfortunately quite often this is not achievable due to oxygen mass transfer limitations. The critical parameter is the oxygen mass transfer coefficient (k_La). It is well known that whereas sufficiently high k_La values may be achieved in small-scale fermenters (which are easily operated in high turbulence regimes), it may be impossible to achieve in large-scale fermenters due to unacceptable power consumption requirements. The problem is particularly critical for high cell density and shear sensitive cultures (e.g., [2,11]). The high cell density is normally required in secondary metabolites production processes to enhance productivity. This leads to

* Corresponding author. Tel.: +351-21-2947804; fax: +351-21-2948385.
E-mail address: rui.oliveira@dq.fct.unl.pt (R. Oliveira).

0959-1524/$ - see front matter © 2004 Elsevier Ltd. All rights reserved.
doi:10.1016/j.jprocont.2004.01.003

Nomenclature

θ	unknown time-varying parameter
μ	specific growth rate
π	specific penicillin production rate
σ	specific substrate consumption rate
τ_1, ζ	time constant and damping coefficient of a second order dynamical equation
τ_2	time constant of first order dynamical equation
μ_{max}	maximum specific growth rate
π_{max}	maximum specific penicillin production rate
C_o	dissolved oxygen concentration
C_o^*	saturation dissolved oxygen concentration
C_o^{SP}	dissolved oxygen concentration set point
$\widehat{C}_o$	estimate of C_o
D	dilution rate
D_{min}	minimum dilution rate
$\hat{\theta}$	estimate of θ
F	total inlet flow rate
F_{out}	outlet flow rate
K_d	autolysis constant
K_h	penicillin hydrolysis rate constant
k_La	volumetric oxygen mass transfer coefficient
K_S	substrate saturation constant
K_X	growth saturation constant
m_o	specific oxygen consumption rate for maintenance
m_s	specific substrate consumption rate for maintenance
$m_{s,max}$	maximum maintenance coefficient
OTR	oxygen transfer rate from gas phase to the liquid phase
P	penicillin concentration
q_o	specific oxygen consumption rate
r_o	volumetric oxygen consumption rate
S	substrate concentration
S_F	substrate concentration in the input feed
t	time
V	working volume
V_d	withdrawn volume
X	biomass concentration
X_{dead}	concentration of dead mycelia
X_{live}	concentration of live mycelia
Y_{PO}	oxygen to penicillin yield
Y_{PS}	substrate to penicillin yield
Y_{SO}	oxygen to substrate yield
Y_{XO}	oxygen to biomass yield
Y_{XS}	substrate to biomass yield

a higher oxygen demand than the reactor's maximum transfer capacity. Therefore, operating strategies to drive processes near maximum oxygen transfer capacity are required. This can be achieved with a DO-based feeding controller that manipulates the addition of the carbon source based on DO measurements [1,3–5].

Many industrial carbon-limited fermentation processes are operated in open-loop. The carbon source feed rate profile is evaluated off-line through optimisation/design procedures (heuristic or model-based) and then implemented on-line with programmable controllers. These optimisation procedures evaluate the optimal feed rate profile that maximises the process output in terms of total product amount or product purity, while obeying to equipment constrains like the maximum k_La. The open-loop operation has some well-known disadvantages related to robustness and uncertainty. For instance, a sudden viscosity increase typical in some mold fermentations may cause a sharp k_La decrease and consequently the process may be brought into oxygen limitation. In such situations the typical response is to decrease manually the carbon source feed rate. If the feed rate is decreased too much, fewer product is produced thus having a negative economic impact. If on the other hand the decrease is not sufficient, the DO concentrations may decrease below the critical level and the run may even be lost. This situation has even higher economic losses attached. Because risks are high, safety is normally preferred over a more risky operation and consequently the feed rate is systematically below its potential maximum value. This is clearly one of such examples where the process productivity could be enhanced by implementing proper automatic closed-loop control.

The main purpose of the present study is to derive an effective closed-loop control solution for driving aerobic fermentation processes near maximum oxygen transfer capacity. The paper is organised in the following way. In Section 2 the relevant methodologies applied are exposed, first the control problem in study is defined, then an adaptive control algorithm is designed and finally the topics of stability and tracking properties are addressed. In Section 3 the adaptive controller is tested with simulations of a penicillin production process. Finally in Section 4 the main conclusions are presented.

2. Methods

2.1. Driving aerobic fermentations near maximum oxygen transfer capacity: problem statement

In stirred-tank aerobic fermentation processes, oxygen transport phenomena occurs among three phases: the gas phase, the liquid phase and the intracellular phase. The

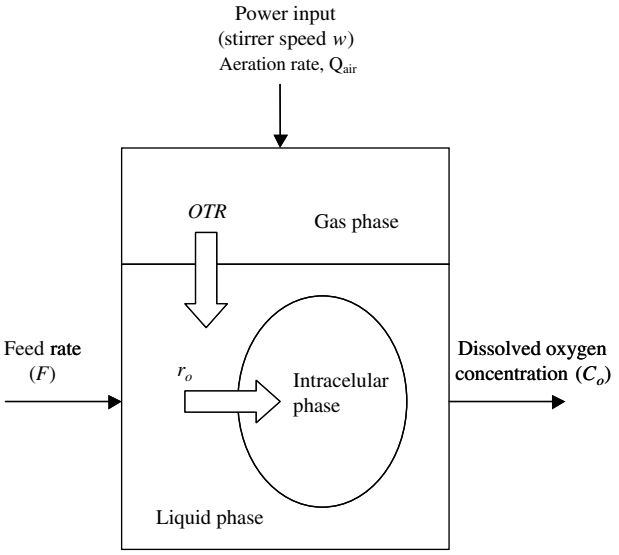

Fig. 1. Oxygen transport in a stirred-tank fermenter.

mass fluxes of this substrate are a chain of three processes as indicated in Fig. 1. Air is sparged into the liquid phase and an oxygen mass flow occurs from air bubbles (gas phase) into the liquid phase. DO flows across the cells' membrane into the intracellular phase. The transport across the cells membrane is a fast process and is never the limiting step in this chain (for this reason it was not indicated in Fig. 1). Finally, oxygen is consumed in the intracellular phase in a set of metabolic reactions for growth, maintenance and product production.

In the perfectly mixed fermenter, the dynamics of oxygen concentration in the liquid phase is described by the following mass balance equation:

$$\frac{dC_o}{dt} = -r_o - DC_o + \mathrm{OTR} \tag{1}$$

being C_o the DO concentration, r_o the oxygen consumption rate, D the dilution rate (defined as $D = F/V$ where F is the total volumetric flow rate into the fermenter and V is the working volume) and OTR the oxygen transfer rate between gas–liquid phases.

The term OTR is normally described by the following mass transfer law:

$$\mathrm{OTR} = k_L a(C_o^* - C_o) \tag{2}$$

being $k_L a$ the volumetric oxygen mass transfer coefficient and C_o^* the oxygen saturation concentration in the liquid phase. The $k_L a$ is a complex function of the fermenter geometry, impeller geometry (as well as number of impellers and impellers positioning), medium composition, as well as of the stirrer speed and inlet airflow rate. The $k_L a$ (and indirectly the OTR) can be manipulated by the stirrer speed w. Hence C_o may be controlled by manipulating the stirrer speed. In practice there is a maximum $k_L a$ (and a maximum OTR) independent of the stirrer speed, normally in the range of 70–900 h^{-1} for industrial fermenters [6]. At this operating point it is impossible to control C_o by manipulating the stirrer speed. The only remaining possibility is to manipulate the term r_o.

The term r_o congregates the microorganisms oxygen metabolic requirements for respirative growth, maintenance and product production. It is a function of biomass concentration and concentrations of several substrates present in the medium, as well as of the microorganisms metabolic state. In carbon-limited processes the metabolism is mainly dependent on the concentration of the carbon source in the liquid phase and indirectly on the feed rate profile. Hence, the term r_o may be manipulated indirectly by the feed rate F. This second alternative for controlling the DO concentration is studied in the present paper.

2.2. Adaptive controller design

Many different control designs could possibly fulfil all desirable prerequisites for this control problem like stability robustness and tracking properties. In the present study a model reference adaptive control (MRAC) design was adopted mainly because it is rather simple and intuitive for the problem in question. The structure of a MRAC system with indirect adaptation is depicted in the diagram of Fig. 2. The main design principle is to force the plant output to follow asymptotically the output of a given reference model that is usually a linear model [7]. When the plant dynamics are only partially known a direct or indirect adaptation scheme is required. In the indirect adaptation strategy the unknown plant parameters are first estimated using the identification model and then the controller parameters are adjusted on the basis of the plant parameters estimates [7]. The identification model is derived directly from the oxygen mass balance equation (Eq. (1)) assuming three assumptions for the physical process:

A1. The microorganisms instantly consume all carbon source material fed to the fermenter, i.e. the accumulation of carbon source may be neglected. This assumption may be relaxed to the assumption that the dynamics of oxygen variation are higher than the dynamics of carbon source concentration variation.

A2. The dilution rate is bounded below

$$D(t) > D_{\min} \quad \forall t \tag{3}$$

A3. The actual oxygen consumption rate can be expressed by the product of the following two time-varying terms,

$$r_o = S_F D(t) Y_{SO}(t) \tag{4}$$

without loss of representativeness of the real system. Eq. (4) means physically that the oxygen

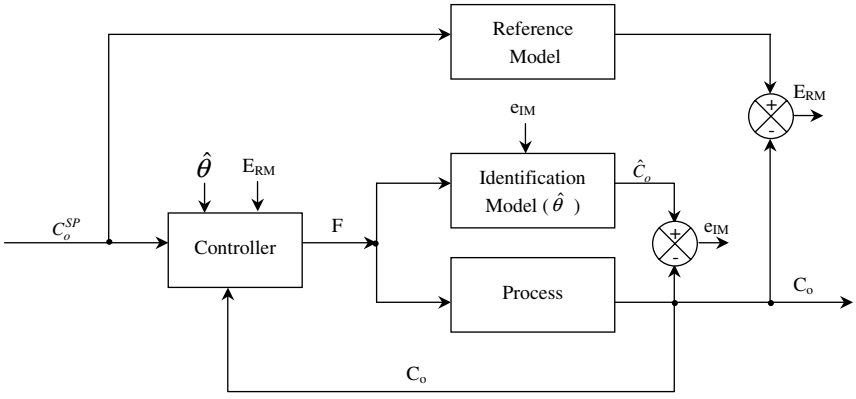

Fig. 2. Model reference adaptive control system with indirect adaptation.

consumption rate is equal to the carbon source consumption rate (defined as the product $S_F D(t)$ where S_F is the carbon source concentration in the feed rate) multiplied by the yield of oxygen to substrate Y_{SO}. Since the intracellular reaction kinetics are complex and inherently dynamic it is necessary to assume that the yield coefficient is a time function.

In Eqs. (1) and (4) all variables are easily accessible on-line at lab-, pilot- and production scales with the exception of the yield coefficient $Y_{SO}(t)$ and possibly the parameter S_F: Oxygen electrodes are widespread in the industry for measuring the DO tension, mass spectrometers (for instance) are employed for 'measuring' the oxygen transfer rate OTR (to be precise OTR is not directly measured but calculated from measurements of the composition of the exhaust gas), and finally the dilution rate D is the result of the feed rate profile, which is the manipulated variable and hence known a priori or is computed by the closed-loop controller. The knowledge of the carbon source concentration in the feed S_F is many times difficult, mainly in fermentations run in complex media where a complex mixture of materials is fed to the fermenter whose raw materials are normally provided by different sources and characterised by a considerable batch-to-batch variability. The uncertainties around the values of S_F and $Y_{SO}(t)$ pose the important constraints for deriving the controller. It is however possible to develop an adaptive scheme that compensates for these uncertainties.

The terms in Eq. (4) may be grouped as $r_o = (D(t))(S_F Y_{SO}(t)) = D(t)\theta(t)$. In this way the oxygen consumption rate is expressed by the product of a known time function with an unknown time function: the first term is $D(t)$ and is known on-line whereas the second term, $\theta(t)$, is unknown. By substituting this definition in Eq. (1) the following identification model equation is obtained:

$$\frac{dC_o}{dt} = -D(t)\theta(t) - D(t)C_o + OTR \tag{5}$$

The term $\theta(t)$ is the only unknown parameter in Eq. (5) and therefore must be estimated. This problem is similar in form to the estimation of reaction kinetics in stirred-tank bioreactors [8]. The observer-based estimator has been widely employed in such cases [8–11]. The application of the observer-based estimator to the system (5) results in the following system of two equations:

$$\frac{d\widehat{C}_o}{dt} = -D(t)\hat{\theta}(t) - D(t)C_o + OTR + (2\zeta/\tau_1 - (dD/dt)/D)(C_o - \widehat{C}_o) \tag{6a}$$

$$\frac{d\hat{\theta}}{dt} = -\frac{(C_o - \widehat{C}_o)}{D(t)\tau_1^2} \tag{6b}$$

being $\hat{\theta}$ and $\widehat{C}_o$ the estimates of C_o and θ respectively. The structure of these equations may not be obvious at first sight but they are motivated by stability reasons. It may be shown that this estimator imposes second order dynamics of convergence of estimated to true values with the proper tuning of the design parameters [12,13]. Provided that $\theta(t)$ is known on-line then we have full knowledge of the process plant. The next step is to define the reference model. For simplicity reasons it was chosen to be a first order dynamics equation for the convergence of DO to the set point:

$$\frac{dC_o}{dt} = \frac{C_o^{SP} - C_o}{\tau_2} \tag{7}$$

being C_o^{SP} the set point and τ_2 the time constant. Finally, by combining Eqs. (5) and (7) and substituting $\theta(t)$ by its estimate the following control equation is obtained:

$$D = \left(OTR - \frac{C_o^{SP} - C_o}{\tau_2}\right)\frac{1}{\hat{\theta}(t) + C_o}, \quad \text{or} \tag{8a}$$

$$F = \left(OTR - \frac{C_o^{SP} - C_o}{\tau_2}\right)\frac{V}{\hat{\theta} + C_o} \tag{8b}$$

The implementation of the control laws (8) implies the integration of the estimator equations (Eqs. (6)). The following initial conditions may be employed

$$\widehat{C}_o(t=0) = C_o(t=0) \quad \text{and} \quad \hat{\theta}(t=0) = \overline{S}_F \overline{Y}_{SO}$$

being $\overline{S}_F$ and $\overline{Y}_{SO}$ estimates of the true parameter values.

2.3. Stability, tracking dynamics and tuning of design parameters

The error system is in this case obtained by substituting Eq. (8a) in the plant Eq. (5). After some rearrangements the following equation is obtained:

$$\frac{d(C_o^{SP} - C_o)}{dt} = -\frac{1}{\tau_2}(C_o^{SP} - C_o) + D(\theta - \hat{\theta}) + \frac{dC_o^{SP}}{dt} \quad (9)$$

This error system is a linear perturbed system. It can be shown to be globally stable if all perturbations are bounded and if the unperturbed part is exponentially stable. The latter condition is verified if the constant time τ_2 is positive. The boundness of the term dC_o^{SP}/dt is normally verified. The boundness of $D(\theta - \hat{\theta})$ depends on the stability of the estimator (6). The global stability of the estimator (6) has been demonstrated in [13]. Furthermore, it has been shown that the estimator (6) imposes second order dynamics of convergence of estimated to true values [12,13]. Subtracting the real process Eq. (5) by Eq. (6a), and combining the resulting equation with (6b) and its derivative yields the following equation:

$$\tau_1^2 \frac{d^2\hat{\theta}}{dt^2} + 2\zeta\tau_1 \frac{d\hat{\theta}}{dt} + \hat{\theta} = \theta \quad (10)$$

which states that the estimated parameter $\hat{\theta}$ converges to the true parameter θ with second order dynamics with time constant τ_1 and damping coefficient ζ [12,13]. If additionally the convergence of (6) is set to be faster than that of (9), i.e. $\tau_1 \ll \tau_2$ then the dynamics of convergence of C_o to the set-point approach that of a first order dynamics equation with time constant time of τ_1. Hence the tuning of the design parameters is in this case rather intuitive. Three parameters must be properly set:

(1) τ_1 and ζ are the time constant and damping coefficient respectively of a second order dynamic response for the estimates of the unknown function $\theta(t)$.
(2) τ_2 is a time constant of a first order dynamic response that defines the speed of convergence of C_o to the set point.

3. Results and discussion

3.1. The process

For the present study, a process model similar to the model described in [14] is used for simulation experiments. The model was developed for an industrial pilot-plant penicillin-G fed-batch fermenter and proved to describe satisfactorily the real process. The model is a structured representation that considers six state variables: concentration of live (X_{live}) and dead (X_{dead}) mycelia, concentration of substrate (S)—which is in fact the lumped concentration of glucose and other carbon compounds, concentration of penicillin (P), concentration of DO (C_o) and working volume (V). The dynamics of the process are described by the set of mass balance equations:

$$\frac{dX_{live}}{dt} = \mu X_{live} - F\frac{X_{live}}{V} - K_d X_{live} \quad (11a)$$

$$\frac{dX_{dead}}{dt} = K_d X_{live} - F\frac{X_{dead}}{V} \quad (11b)$$

$$\frac{dS}{dt} = -\sigma X_{live} - F\frac{S - S_F}{V} \quad (11c)$$

$$\frac{dP}{dt} = \pi X_{live} - F\frac{P}{V} - K_h P \quad (11d)$$

$$\frac{dC_o}{dt} = -q_o X_{live} - F\frac{C_o}{V} + k_L a(C_o^* - C_o) \quad (11e)$$

$$\frac{dV}{dt} = F - F_{out} \quad (11f)$$

The specific kinetic rates μ, K_d, σ, π and q_o are described by Monod-type relationships:

$$\mu = \frac{\mu_{max} S}{K_X X_{live} + S} \quad (11g)$$

$$\pi = \frac{\pi_{max} S}{K_P + S} \quad (11h)$$

$$m_s = \frac{m_{s,max} S}{K_S + S} \quad (11i)$$

$$\sigma = \frac{\mu}{Y_{XS}} + \frac{\pi}{Y_{PS}} + \zeta \quad (11j)$$

$$q_o = \frac{\mu}{Y_{XO}} + \frac{\pi}{Y_{PO}} + m_o \quad (11k)$$

The model parameters employed are listed in Table 1. The model described in [14] did not include the oxygen equations (Eqs. (11e) and (11k)) (in the original study,

Table 1
Penicillin model (Eq. (13)) parameters

Parameter	Value
μ_{max}	0.13 h^{-1}
K_X	0.13 g/l
π_{max}	0.011 h^{-1}
K_h	0.003 h^{-1}
K_d	0.006 h^{-1}
K_P	0.0001 g/l
m_s	0.02 h^{-1}
K_s	0.0001 g/l
Y_{XS}	0.52
Y_{PS}	1.0
Y_{XO}	1.406
Y_{PO}	5.85
m_o	0.022 h^{-1}
$k_L a$	175 h^{-1}
C_o^*	7 mg/l

the oxygen concentration was never limiting). Since in this work the oxygen concentration is the key control quantity, Eqs. (11e) and (11k) were added to the original set of equations. These equations and corresponding parameters were taken from Pirt [15].

For the set of simulation experiments performed, the same process operating conditions described in [14] were adopted:

1. The pilot scale fermenter is initially charged with $V(t=0)=600$ l of fermentation medium composed by corn steep liquor and sugar syrup.
2. The medium charged initially had a concentration of glucose of $S(t=0)=4$ g/l (glucose is the most important carbon source).
3. Feeding of glucose syrup starts after an initial batch period of 10 h with a glucose concentration of $S_F=240$ g/l.
4. Scheduled discharges are performed. For simplicity we consider that 100 l medium is withdrawn each time V equals or exceeds the value of 950 l.
5. The fermentation duration is 240 h.

The process performance (J) is measured by the total penicillin produced with units of kilograms quantified by the equation:

$$J = P(t=240)V(t=240) + \sum_{i=1}^{N_d} P(t_i)V_d(t_i) \qquad (12)$$

being N_d the number of discharges performed at times t_i and V_d the withdrawn volume of the medium (for the present case V_d is always 100 l).

3.1.1. The adaptive controller implementation

The controller was implemented within of a scheduled operation scheme that considers three distinct phases:

1. Batch phase: In this phase the mold consumes the initially charged glucose. No glucose is fed to the fermenter during this phase that takes the first 10 cultivation hours.

   $F=0 \quad t \leqslant 10$ h

2. Open-loop phase: An exponential feed rate profile is implemented until the oxygen concentration reaches 35% of saturation.

   $F(t)=6-2e^{(10-t)/25} \quad t>10 \quad \text{and} \quad C_o \geqslant 1.05C_o^{SP}$

3. Closed-loop phase: Once the oxygen concentration decreases below 35% of saturation, the adaptive controller starts controlling C_o to the set point $C_o^{SP}=0.3C_o^*$ (30% of saturation).

3.1.2. Open-loop operation

In large scale fermenters oxygen availability will ultimately dictate the total amount of penicillin produced. The carbon source feed rate profile must be carefully chosen so that oxygen is never limiting. The process was simulated with the following two feed functions:

$$\text{feed1:} \quad F=0 \quad t \leqslant 10 \text{ h}, \qquad F=4-2e^{-t/25} \quad t>10 \text{ h}.$$

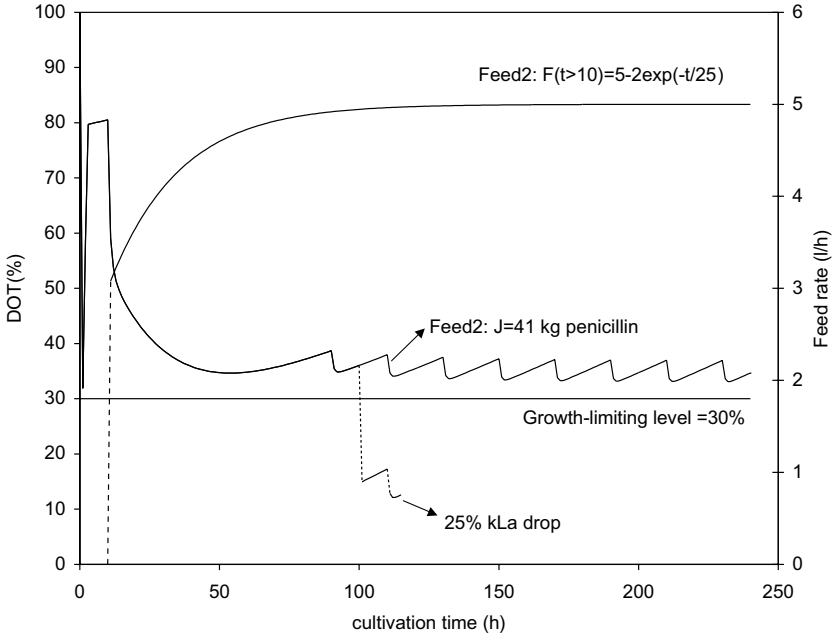

Fig. 3. Effect of the feed rate in the penicillin productivity for the case of open-loop operation: exponential feed rate feed2 and corresponding DO profile.

feed2: $F = 0 \quad t \leqslant 10$ h,

$F = 5 - 3e^{-t/25} \quad t > 10$ h

With feed1, the oxygen concentration approaches the critical limiting level (DO = 30% of saturation) as the cultivation progresses in time but stays above this level (not shown in the pictures). The total penicillin produced using feed1 was $J = 33$ kg. In principle this total amount can be increased if more sugar is fed to the fermenter. As shown in Fig. 3 using feed2 the total penicillin produced increased to $J = 41$ kg. Although this represents a significant improvement in penicillin production, the DO is now much closer to the critical level. Since the process is operated in open-loop, the feed2 strategy may be a risky choice because the process becomes very sensitive to disturbances. In penicillin fermentations a sudden viscosity increase may cause a sharp $k_L a$ decrease. This situation is illustrated in Fig. 3. A 25% $k_L a$ decrease at time $t = 100$ h yields a sharp decrease of DO below 10% of saturation.

3.1.3. Adaptive controller

With this background, one could anticipate that the proposed controller could increase product production and improve safety and robustness. The main results are shown in Fig. 4a–c. Fig. 4a shows the time evolution of the glucose feed rate during the three process phases and the corresponding DO profile. It may be seen that both the feed as well as the DO signals exhibit small oscillations at time ca. 20 h. These oscillations refer to the transition between open-loop to closed-loop phases. Apart from these small oscillations the controller was able to control very efficiently the concentration of DO to the desired set-point level. The total amount of penicillin produced was $J = 45$ kg. It represents 9.8%

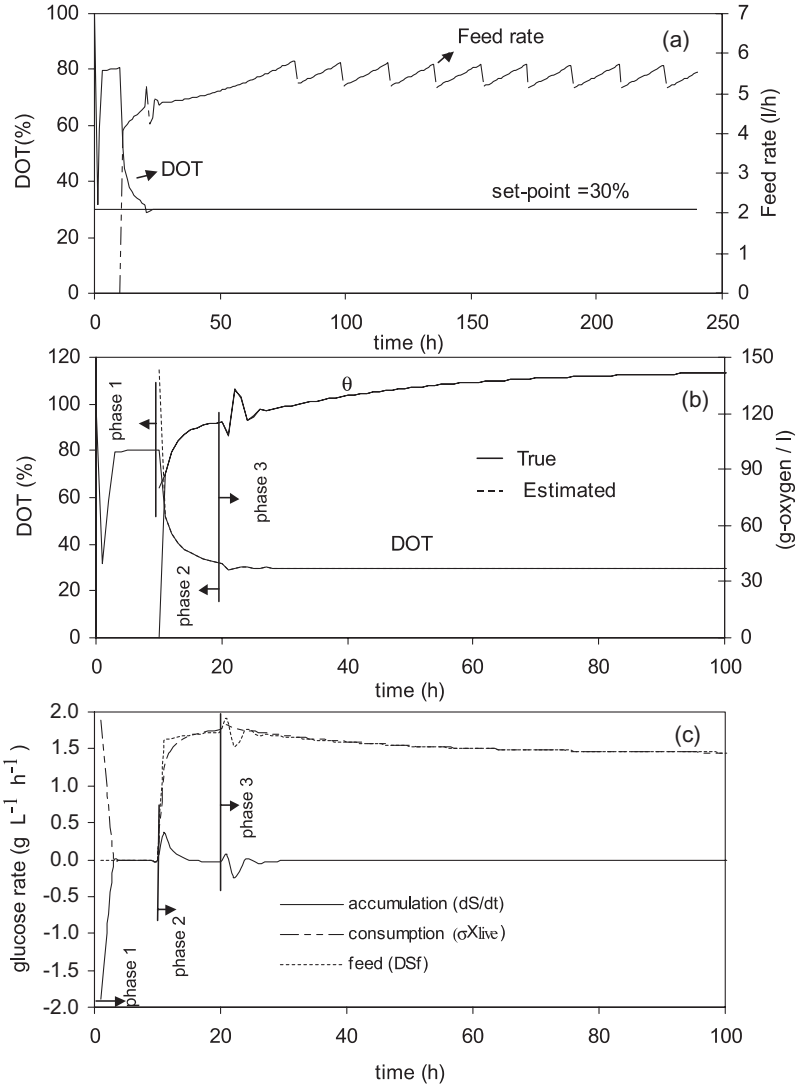

Fig. 4. Adaptive control results with controller parameters $\tau_1 = 0.001$ h, $\tau_2 = 0.001$ h and $\zeta = 1.5$: (a) DO concentration and feed rate, (b) estimator results for DOT and θ, (c) glucose flows along the process trajectory.

increase in relation to the open-loop operation using feed2 (the more risky hypothesis) and 36.4% increase in relation to the open-loop operation using feed1 (the safer hypothesis).

The performance of the estimator (6) may be assessed from the analysis of Fig. 4b. Fig. 4b shows both DOT and $\theta(t)$ estimation results. Both variables were estimated very accurately in the whole time domain. The "true" θ value was calculated by the expression $\theta(t) = q_o X_{live}/D$. As may be seen in Fig. 4b $\theta(t)$ exhibited some oscillation during the transition between open-loop (phase 2) to closed-loop (phase 3) phases. These oscillations were reflected in the control action and may be explained by the fact that assumption A1 does not hold true, i.e. not all sugar fed is instantly consumed. Fig. 4c plots the glucose flows along the process trajectory. It may be concluded that the accumulation term is relevant in the initial batch phase (as expected) but negligible in the open-loop and close-loop phases in comparison to the consumption and input feed rate terms.

3.1.4. Testing the controller in the presence of noise

To characterise the behaviour of the controller in the presence of noise in the measured signals, white noise was added to both the measured oxygen concentration (with $\sigma = 0.12$ mg/l) and the oxygen transfer rate (with $\sigma = 0.012\ g\,h^{-1}\,l^{-1}$). The results are shown in Fig. 5a and b. It may be seen in these pictures that the algorithm worked satisfactorily in the presence of noise and did not amplify it. The true process DOT is almost insensitive to the noise. Actually the estimator behaves like a filter because it introduces a time delay in the estimation of both DOT and θ. Finally it is important to mention that the usual noise associated with oxygen concentration and oxygen transfer rate measurements can be easily filtered. The application of, for instance, a moving average window technique or a first order filter with high frequency sampling yields normally good results. In principle the usual noise attached to these variables will not pose severe difficulties for the implementation of the controller discussed here.

3.1.5. Response to process loads

The response of the adaptive controller to $k_L a$ step changes for different controller settings is shown in Fig. 6. The $k_L a$ decreased from 175 to 131 h^{-1} at time $t = 100$ and was restored to the initial value at $t = 120$ h. The impact of these disturbances is relevant but the controller managed to bring the DOT to the corresponding

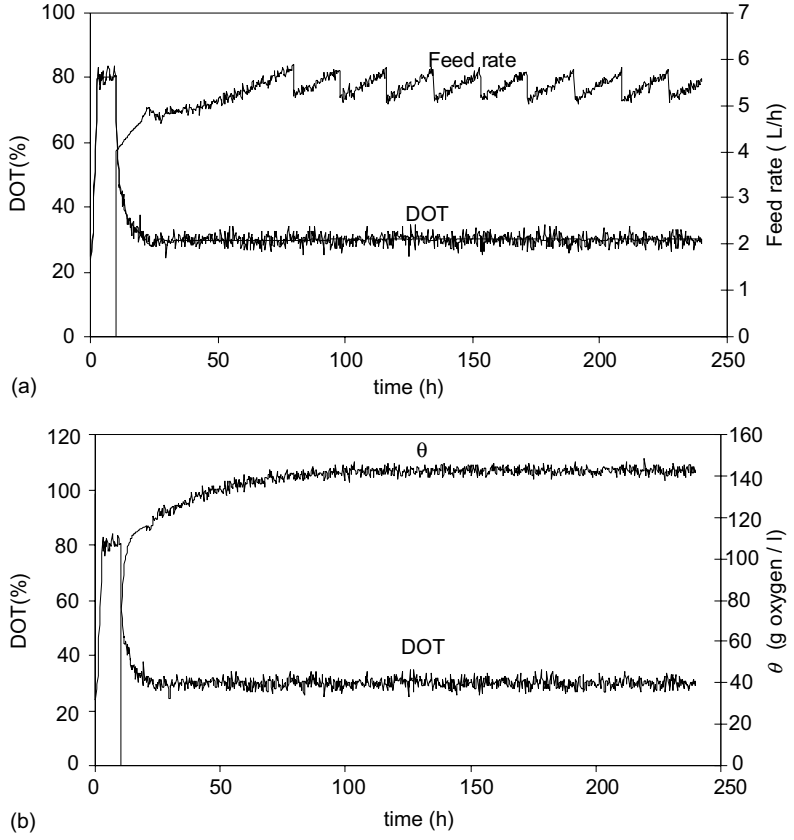

Fig. 5. Adaptive control results with white noise in DOT ($\sigma = 1.17 \times 10^{-4}$) and OTR ($\sigma = 1.20 \times 10^{-2}$) with controller parameters $\tau_1 = 0.001$ h, $\tau_2 = 0.001$ h and $\zeta = 1.5$: (a) DO concentration and feed rate, (b) DOT and θ estimation results.

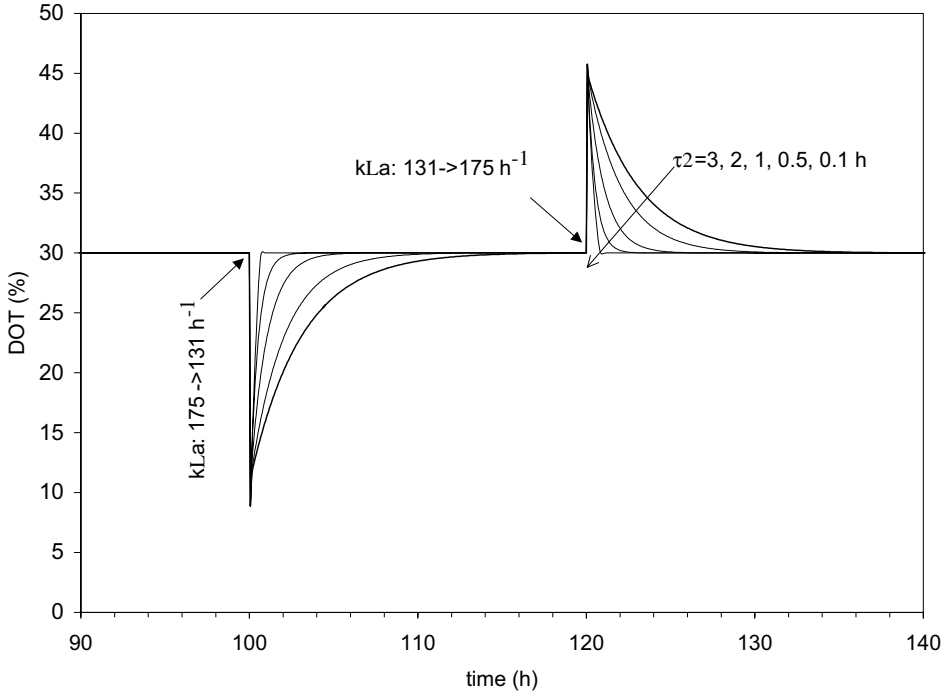

Fig. 6. Response of the adaptive controller to k_La step changes for different controller parameters: $\tau_1 = 1 \times 10^{-4}$ h, $\zeta = 1.5$ and $\tau_2 = 3$, 2, 1, 0.5 and 0.1 h.

set point with characteristic first order dynamics in conformity with the theoretical results presented in Section 2.3. As mentioned previously three controller parameters must be properly set. Two of these parameters belong to the estimator. They are the time constant, τ_1, and the damping coefficient, ζ, characteristic of a second order system that defines, in this case, the dynamics of convergence to the true parameter $\theta(t)$ (Eq. (10)). The other parameter is a time constant, τ_2, of a first order dynamic response that defines the speed of convergence of C_o to the set point. The tuning of the design parameters is in this case rather intuitive. The parameter τ_1 sets the speed of convergence of the estimator while ζ controls the oscillatory behaviour. Oscillations may be avoided if $\zeta \geqslant 1$. The parameter τ_2 sets the speed of convergence of the control variable to the set point. The most important rule for tuning these parameters is that the speed of the estimator should be higher than the speed of controller, i.e. $\tau_2 \gg \tau_1$, otherwise uncharacteristic oscillations are observed due to the interference of the θ estimation error as indicated in Eq. (9). Fig. 6 shows the controller response to the same load for the settings $\tau_1 = 1 \times 10^{-4}$ h^{-1}, $\zeta = 1.5$ and $\tau_2 = 3$, 2, 1, 0.5, 0.1 h^{-1}. In this case $\tau_2 \gg \tau_1$ is verified and therefore typical first order responses were produced. It can also be observed that the initial amplitude of DOT deviations is higher when k_La is decreasing (first perturbation) than when k_La is increasing (second perturbation). It was verified that the first perturbation, when k_La decreased from 175 to 131 h^{-1}, led to the controller saturation with $D = D_{min}$ (assumption A2, Eq. (3)) that was 2.5×10^{-3} h^{-1} in this case.

4. Conclusions

In this work we presented an adaptive control algorithm designed specifically for driving aerobic fermentations near maximum oxygen transfer capacity. The controller is applicable to aerobic fermentations run in stirred-tank bioreactors under carbon source limitation. The control problem studied is directly linked to economical issues and is of significant practical relevance. It was demonstrated with simulation studies that in the case of a penicillin production process, relevant productivity improvements could be achieved. The same kind of results could be anticipated in high cell density processes with both growth and non-growth associated product production kinetics. In the particular case of animal cell cultures this controller could be of great practical usability since they are very sensitive to the agitation.

The controller presented requires two on-line measurements that are currently standard in the industry: DO electrodes and the MS or other device for measuring concentration of oxygen in the outlet gas stream. The two variables can be measured accurately and reliably and pose no problems for the practical applicability of the control system.

The controller has a physical basis but does not require detailed knowledge about mixture compositions neither about kinetics or kinetic parameters. In particular the controller could be applied to both defined and complex media cultivation processes with unknown composition.

References

[1] J.D. Chung, Design of metabolic feed controllers: application to high-density fermentations of *Pichia pastoris*, Biotechnology and Bioengineering 68 (3) (2000) 298–307.
[2] L. Simon, M.N. Karim, Identification and control of DO in hybridoma cell culture in a shear sensitive environment, Biotechnology Progress 17 (4) (2002) 634–642.
[3] M. Akesson, P. Hagander, J.P. Axelsson, Avoiding acetate accumulation in *Escherichia coli* cultures using feedback control of glucose feeding, Biotechnology and Bioengineering 73 (3) (2001) 223–230.
[4] M. Akesson, E.N. Karlsson, P. Hagander, J.P. Axelsson, A. Tocaj, On-line detection of acetate formation in *Escherichia coli* cultures using dissolved oxygen responses to feed transients, Biotechnology and Bioengineering 64 (5) (1999) 590–598.
[5] B. Kupcsulik, B. Sevella, A. Ballagi, J. Kozma, Evaluation of three methanol feed strategies for recombinant *Pichia pastoris* Mut(s) fermentation, Acta Alimentaria 30 (1) (2001) 99–111.
[6] P.M. Doran, Bioprocess Engineering Principles, Academic Press, UK, 1995.
[7] K.S. Narendra, A.M. Annaswamy, Stable Adaptive Systems, Prentice-Hall, Englewood Cliffs, NJ, 1989.
[8] G. Bastin, D. Dochain, On-Line Estimation and Adaptive Control of Bioreactors, Elsevier, Amsterdam, 1990.
[9] Y. Pomerleau, M. Perrier, Estimation of multiple specific growth rates in bioprocesses, AIChE Journal 36 (2) (1990) 207–215.
[10] J.E. Claes, J.F. Van Impe, On-line estimation of the specific growth rate based on viable biomass measurements: experimental validation, Bioprocess Engineering 21 (5) (1999) 389–395.
[11] E.J. November, J.F. Van Impe, The tuning of a model-based estimator for the specific growth rate of *Candida utililis*, Bioprocess and Biosystems Engineering 25 (1) (2002) 1–12.
[12] R. Oliveira, E.C. Ferreira, F. Oliveira, S. Feyo de Azevedo, A study on the convergence of observer-based kinetic estimators in fed-batch fermentations, Journal of Process Control 6 (6) (1996) 367–371.
[13] R. Oliveira, E.C. Ferreira, S. Feyo de Azevedo, Stability and dynamics of convergence of observer-based kinetics estimators, Journal of Process Control 12 (2002) 311–323.
[14] J.C. Menezes, S.S. Alves, J.M. Lemos, S. Feyo de Azevedo, Mathematical modelling of industrial pilot-plant penicillin-G fed-batch fermentations, Journal of Chemical Technology and Biotechnology 61 (1994) 123–138.
[15] S.J. Pirt, The Penicillin Fermentation: A Model for Secondary Metabolite Production, Pirtferm Papers, Series A, Pirtferm Limited, 1994.